JJBS

Volume 15, Number 5,December 2022
ISSN 1995-6673
Pages 855 – 868
https://doi.org/10.54319/jjbs/150515

Jordan Journal of Biological Sciences

Bioethanol Production from Biologically Pretreated *Prosopis africana* Pods using *Pichia kudriavzevii* SY4

Amina Ahmed El-Imam[1,2], Eromosele Ighalo[2,*], Mardhiyah Sanusi[2], Mushafau Adebayo Oke[3], Patricia Folakemi Omojasola[2]

[1]*Department of Plant and Microbial Biology, North Carolina State University, 27607 USA* [2]*Microbiology Department, The Life Sciences Faculty, University of Ilorin.;* [3]*Independent Researcher, Edmonton, AB, Canada.*

Received: July 30, 2022; Revised: September 29, 2022; Accepted: October 2, 2022

Abstract

High costs and ethical issues have prompted research into novel non-food feedstocks for the fermentation-based manufacture of sustainable fuels. In this study, *Prosopis africana* pods (PAP), an underutilized substrate, was examined for its ability to produce bioethanol. The biomass was pretreated with four mushrooms to delignify it and enhance hydrolysis. A scanning electron microscopy (SEM) was performed on raw and pretreated PAP. The optimum hydrolysis conditions for the pretreated biomass were then determined using the Design of Experiment (DOE) approach. The acid type (HNO_3 and H_3PO_4), concentration (1 %, 3 % and 5 %), solid loading (SL; 5 %, 10 % and 20 %) and contact time (15, 30 and 60 minutes) were optimized using a full-factorial design. The most tolerant yeast isolate from different sources was then molecularly identified after being tested for ethanol tolerance. A half-factorial design was used to screen the fermentation factors, and the Box-Behnken design was used to optimize the relevant components. *Ganoderma lucidum* showed the most luxurious growth during PAP pretreatment and SEM revealed reduction in biomass crystallinity. The hydrolysis conditions of 5 % HNO_3, 20 % SL and 15 minutes contact time were optimal, producing 43.37 ± 0.35 g/L of reducing sugars. The most ethanol-tolerant strain, identified as *Pichia kudriavzevii* SY4, produced 38.26 g/L bioethanol concentration after RSM optimisation. Similarly, optimisation raised bioethanol concentrations from 26.62 ± 0.00 to 38.26 ± 0.18 g/L, a 43.73 % increase. This work is the first report on utilising *Prosopis africana* pods in bioethanol production.

Keywords: Bioethanol, Fermentation, Hydrolysis, Optimisation, *Prosopis africana*, Response Surface Methodology.

1. Introduction

Increasing industrial activities and rapid population increase have caused a boom in energy demand (Raina *et al*., 2020). With more than four-fifths of the global energy market, fossil-derived fuels constitute the main energy source (Branco *et al*., 2019). Over-exploitation has rapidly depleted fossil resources, raising major environmental issues (Milano *et al*., 2016). Consequently, research interest in alternative energy sources has increased drastically (Awoyale and Lokhat, 2019; Rezania *et al*., 2019). One such alternative is biofuels, which can significantly reduce fossil fuel dependence and lower greenhouse gas emissions (Braz *et al*., 2019). The most common biofuel is bioethanol, with 115 billion liters produced in 2019 and it is anticipated to reach 119 billion liters in 2023 (IEA, 2019; Ahmed El-Imam *et al*., 2019).

According to the International Energy Agency (IEA), biofuels should account for 27 % of global transportation fuels by 2050 to satisfy global energy-related CO_2 targets (Ghani *et al*., 2019). First-generation (1G) bioethanol production from carbohydrates (Ibeto *et al*., 2011) like corn starch and sugarcane sugars resulted in the ethical problem of using arable lands to cultivate biofuel crops (Adelabu *et al*., 2018), a negative impact on biodiversity, and contributed to deforestation and desertification (Gerbens-Leenes, 2017; Awoyale and Lokhat, 2021). Thus, the focus shifted to second-generation (2G) or renewable bioethanol, produced by the hydrolysis and fermentation of several feedstocks, including lignocellulosic biomass and industrial and food processing wastes (Ahmed El-Imam *et al*., 2019).

The Russia-Ukraine war, which started in February 2022, has resulted in global spikes in the prices of food and fossil energy sources. Thus, the USA is considering expanding corn-based ethanol production (Gustin, 2022) to reduce dependence on imported oil and lower domestic gasoline prices. However, expanding 1G bioethanol is now even more discouraged due to currently surging food insecurity. An alternative raw material, lignocellulosic biomass, is abundant in nature and affordable, and its utilization in 2G fuel production assures a renewable, self-sufficient and secure supply (Bhatia *et al*., 2017; Branco *et al*., 2019; Wuryantoro *et al*., 2021) at more affordable prices.

Common lignocellulosic materials include agricultural wastes like straw and stover, food processing wastes like bagasse, brans, and pods, and dedicated energy crops like switchgrass and *Miscanthus* sp. These biomasses are composed structurally of hemicellulose, cellulose, and lignin bonded into a stiff matrix that resists hydrolysis into

* Corresponding author. e-mail: eromoseleighalo@gmail.com.

simple sugars and calls for pretreatment techniques (Malik *et al*, 2020; Yildirim *et al*., 2021). The African mesquite (*Prosopis africana*) tree is a perennial leguminous tree found throughout East and West Africa's savanna regions. Its seeds are used to make food condiments, with the empty pods being frequently discarded indiscriminately. These pods are rich in carbohydrates, proteins, and other nutrients, making them ideal for microbial growth and conversion into important and useful products (Pasiecznik *et al*., 2001; Oni *et al*., 2020).

Before utilization, biomass needs to be pretreated, and more than one pretreatment type is commonly employed. Physical pretreatment includes methods like microwave irradiation, ultrasound pretreatment, and size reduction operations. Ionic liquid delignification and acid or alkaline pretreatment are examples of chemical pretreatment methods, whereas CO_2, SO_2, or steam explosion and liquid hot water treatment are examples of physicochemical pretreatment methods (Karimi *et al*., 2013; Beig *et al*., 2021; Yildirim *et al*., 2021). The last pretreatment method is biological, which entails utilizing white-rot fungi and other microbes to break down the dense structure of lignocellulose while leaving the sugars, which can then be hydrolyzed and fermented.

Pretreatment is the most expensive phase of biofuel production, contributing up to 30 % of the total cost (Beig *et al*., 2021). Its advantages include low cost, low severity (Taufikurahman *et al*., 2020), low energy and additive requirements, and the absence of fermentation inhibitors, toxic end-products, and effluents. Biological pretreatment frequently utilizes the white-rot fungi *Trametes versicolor*, *Pleurotus* sp., *Phanerochaete chrysosporium*, and *Lentinus squarrosulus* to delignify the biomass (Sindhu *et al*., 2016; Ahmed El-Imam *et al*., 2021). The residual carbohydrates are then readily depolymerized into sugars and fermented into bioethanol.

Bioethanol production has been reported using *Prosopis juliflora* pods (da Silva *et al*., 2011), but there are no reports using *P. africana* pods (PAP). Here, we report bioethanol production from PAP by optimizing the hydrolysis and fermentation stages using the Full Factorial Design (FFD) and the Response Surface Methodology (RSM), respectively. DOE strategy was employed because it is a multivariate technique widely used to develop products and processes. For the first time, these discoveries point to the optimum conditions for the fermentation-based ethanol generation from the African mesquite tree's pods.

2. Materials and Methods

2.1. Isolation of microorganisms

Yeasts were isolated from different sources (palm wine, sugarcane bagasse, and spoilt oranges) using yeast extract peptone dextrose (YPD) agar (peptone 20 g/L, yeast extract 10 g/L, dextrose 20 g/L, and agar 15 g/L) and incubating at 30 °C for three days. Distinct colonies were selected, purified and pure colonies were maintained on Potato Dextrose Agar (Himedia, India) slants and stored at 4 °C pending use.

2.2. PAP collection and biological pretreatment

Mature pods were obtained from the University of Ilorin campus in North-Central Nigeria. They were dried and milled with a typical locally-fabricated petrol-operated Burr-plate mill and sieved with a 50 mesh sieve. The pods were pretreated biologically using *Ganoderma lucidum*, *Pleurotus eryngii*, *Pleurotus pulmonarius,* and *Hypsizygus ulmarius* obtained from TLC mushrooms Limited, Nigeria. These fungi were chosen because research has shown that members of white rot fungi are the most efficient organisms for delignification as they produce different kinds of lignin-modifying enzymes such as laccase (Lac), manganese peroxidase (MnP), lignin peroxidase (LiP), and versatile peroxidase (VP) (Manavalan *et al*., 2015; Ahmed El-Imam *et al*., 2021). A total of six hundred grams (600 g) of the substrate were put into jute bags, which were then weighed after being moistened to a moisture content of 52 % (w/w) using sterile distilled water. The bags and their contents were sterilized for 30 minutes at 121 °C, and when appropriate, the final moisture contents were adjusted to 52 percent. After being allowed to cool, the bags were inoculated in triplicates with 8 % w/dw of single mushroom spawn and incubated for 21 days at 25 °C ± 2 °C in the dark (Rani *et al*., 2008). The treatment with the most extensive mushroom colonization was selected for hydrolysis and fermentation.

2.3. Analysis of pretreated PAP surface

The structure of the PAP and biologically processed PAP biomasses were examined using Scanning Electron Microscopy (SEM). The samples were placed on carbon tapes and carbon-coated using a carbon coater. Then, using a Phenom ProX desktop SEM (Phenom-World, Netherlands) with a magnification range of 20 – 100,000 x, element detection range of C–Am, and acceleration voltage of 10 kV, the surface characteristics and microstructure of the PAP fibers were examined.

2.4. Ethanol tolerance test

An ethanol tolerance test was performed following a modification of the method described (Iticha, 2016). Using a Neubauer hemocytometer, cell concentrations of suspensions of the isolates were determined, and the cells were inoculated at 1.0×10^7 cells/ml into duplicate 10 ml volumes of a 10 % ethanol (v/v) solution in YPD broth. The OD_{600} of the cultures was measured after three days of incubation at 30 °C. The strain that was most tolerant of ethanol was the one with the highest turbidity.

2.5. Molecular identification of yeast isolate

The most ethanol tolerant isolate was molecularly identified by performing nucleotide sequencing of ITS regions 1 and 2. Genomic DNA was extracted as described (Atalla *et al.,* 2019; Atalla *et al.*, 2020a). The internal transcribed spacer (ITS) 1 and 2 regions were amplified by polymerase chain reaction (PCR) using the primer pairs ITS4: 5-TCCTCCGCTTATTGATATGC-3 and ITS5: 5-GGAAGTAAAAGTCGTAACAAGG-3 (Hamed *et al.,* 2015; Atalla *et al*., 2020b). Initial denaturation at 95 °C for 5 minutes, followed by 35 cycles of denaturation at 95 °C for 1 minute, annealing at 53 °C for 1 minute, extension at 72 °C for 1 minute, and a final extension at 72 °C for 7 minutes, were the PCR conditions. Amplified fragments were visualized on safe view-stained 1.5 % agarose electrophoresis gels and sequenced. Sequence homology was used to identify the strain by comparing the sequences to entries in the NCBI database. After that, phylogenetic analysis was carried out, and the data were clustered using

the neighbor-joining and maximum likelihood methods using the Molecular Evolutionary Genetics Analysis (MEGA) program version 5.2 (Tamura *et al*., 2011).

2.6. Optimisation of Dilute Acid Hydrolysis and reducing sugars estimation

A 3^4 factorial design experiment with 4 factors and 3 levels (Table 1) was conducted to optimize dilute acid hydrolysis of the biologically-pretreated PAP. All hydrolysis were performed in duplicates at 121 ˚C and 15 psi using an autoclave. The total of 108 runs and resultant sugar concentrations are presented in Supplementary Table 1.

The effects of the factors on reducing sugar concentrations were investigated by the second-order polynomial shown below:

$$Y = \alpha_0 + \alpha_1X_1 + \alpha_2X_2 + \alpha_3X_3 + \alpha_4X_4 + \alpha_{1,2}X_1X_2 + \alpha_{1,3}X_1X_3 + \alpha_{1,4}X_1X_4 + \alpha_{2,3}X_2X_3 + \alpha_{2,4}X_2X_4 + \alpha_{3,4}X_3X_4 \quad (1)$$

Where Y is the predicted response (reducing sugars concentration, g/L), α_0 to $\alpha_{3,4}$ are the regression coefficients, and X_1, X_2, X_3 and X_4 are the factors.

Table 1. Independent factors and levels evaluated in the full factorial experimental design in the dilute acid hydrolysis of *Prosopis africana* pods (PAP)

Factors	Levels		
	- 1	0	+ 1
Acid type: (HNO3 and H3PO4) (X1)	-	-	-
Acid conc. (v/v) (X2)	1 %	3 %	5 %
SLR (w/v) (X3)	5 %	10 %	20 %
Hydrolysis time (mins) (X4)	15	30	60

Using Whatman No. 1 filter paper, the hydrolysis slurries were filtered, and the filtrate's pH was then raised to pH 5.5. The DNS method was used to estimate the amount of reducing sugars in the hydrolysate following the method described by Sana *et al*. (2017). 3 ml of DNS reagent was combined with precisely 1 ml of the hydrolysate. Standard and blank samples were created so that the outcomes could be compared. Instead of the hydrolysate, the blank sample included 1 ml of distilled water. Different concentrations (0.02-0.1 %) of glucose standard solutions were prepared. The tubes were incubated at 100 ˚C using a waterbath for 15 minutes. The samples were examined by a UV-spectrophotometer at a wavelength of 540 nm after cooling and the amount of reducing sugars present in the hydrolysate was estimated from a glucose standard curve (Supplementary Figure 1).

2.7. Fermentation

2.7.1. Fermentation conditions

The most ethanol-tolerant yeast strain was employed in the fermentation of the YPD medium and the Dilute Acid Hydrolysate (DAH). The DAH was filter-sterilized using a 0.2 µm Stericup® filter. Triplicate 250 ml flasks containing 25 ml of the medium at pH 5.5 were pitched at stated concentrations and incubated in various conditions (Ahmed El-Imam, 2017; Ahmed El-Imam *et al*., 2019).

2.7.2. Screening of variables using half-factorial experimental design

To ascertain the baseline yield of the given microbe-substrate combination, a preliminary experiment was conducted. The flasks were agitated at 140 rpm for four days at 30 °C with a cell concentration of 1 x 10^7 yeast cells/ml (Adelabu *et al*., 2017; Chang *et al*., 2018). Samples were taken every 24 hours, and the amounts of ethanol and residual glucose were determined.

A two-level and five-factor (2^{5-1}) design was then employed to evaluate five factors and identify which significantly impacted bioethanol production. The range for the fermentation parameters was based on earlier studies (Adelabu *et al*., 2017; Chang *et al*., 2018) and the experimental design is shown in Table 2.

Table 2: Independent factors and levels for half-factorial experimental design in the fermentation of dilute acid hydrolysates of *Prosopis africana* pods (PAP) for ethanol production

Factors	Levels	
	Low	High
Temperature (°C) (X1)	25	35
Inoculum size (cells/ml) (X2)	1 × 105	1 × 107
pH (X3)	3	7
Agitation speed (rpm) (X4)	0	140
Incubation period (h) (X5)	24	96

In order to determine the ideal fermentation conditions, the experimental findings were fitted to the second-order polynomial equation shown below. This way, the influence of the factors and the multiple interaction effects on the observed response were investigated.

$$Y = \alpha_0 + \alpha_1X_1 + \alpha_2X_2 + \alpha_3X_3 + \alpha_4X_4 + \alpha_4X_5 \quad (2)$$

Where Y is the predicted ethanol concentration, X_1, X_2, X_3, X_4, and X_5 are the factors, and α_0 to $\alpha_{4,5}$ are the regression coefficients.

2.7.3. Response Surface Optimisation of factors

To optimize factors identified as significant from the half-factorial screening, Box-Behnken Design (BBD) was used (Table 3).

Table 3: Independent factors and levels for BBD

Factors	Levels		
	-1	0	1
pH	3	5	7
Agitation speed (rpm)	0	70	140
Incubation period (h)	24	60	96

The polynomial quadratic equation was used to evaluate the effects of each factor on the response (Xie *et al*., 2013):

$$Y_i = b_0 + \sum b_iX_j + \sum b_{ij}X_iX_j + \sum b_{ii}X^2_i + e_i \quad (3)$$

Yi is the dependent variable, or predicted response (ethanol concentration, g/L), and Xi and Xj are the independent variables. b*i* and b*ij* are the single and interaction effect coefficients, respectively, and *ei* is the error term.

2.7.4. Bioethanol estimation

The potassium dichromate technique described by Koshy *et al*. (2014) was used to quantitatively estimate the concentration of bioethanol in the hydrolysate. Exactly 30 µl of test sample were taken out of the fermentation broth and placed in test tubes. The volume was then increased to 500 µl with distilled water. 1 ml and 2 ml of potassium dichromate and 2 N NaOH reagents were added to each tube respectively. 30 µl of distilled water, 1 ml of potassium dichromate reagent, and 2 ml of 2 N NaOH reagent made up the blank solution. The tubes were

incubated for 30 minutes at 50 ˚C. After cooling, a spectrophotometer was used to measure the absorbance at 600 nm. Based on an ethanol standard curve (Supplementary Figure 2), the amount of bioethanol in the hydrolysate was determined.

2.8. Statistical analysis

Minitab software version 17 was used to conduct an analysis of variance (ANOVA) to determine the impact of the variables under investigation. Significant factors were those with p values < 0.05.

3. Results And Discussion

3.1. Isolation, screening, and molecular identification of yeast isolates

Of sixteen (16) yeast isolates obtained, strain SY4, which showed the most prolific growth in ethanol concentrations of 10 %, was identified using molecular techniques. It had a 99.04 % similarity to *Pichia kudriavzevii* strain ATCC 6258 with accession number NR_131315.1. A phylogenetic tree shows the position of SY4 (Figure 1).

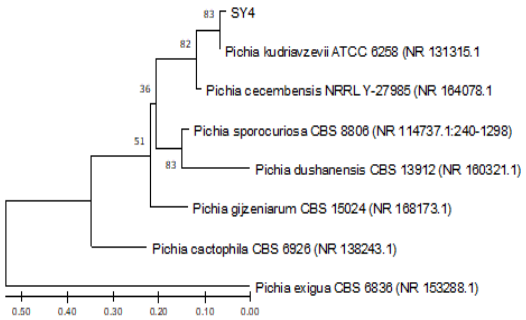

Figure 1: The phylogenetic relationships between yeast isolate SY4 and other closely related species using combined ITS 1 and 2 sequencing analyses. The percentages of replicate trees in which the related taxa clustered together in the bootstrap test are next to the branches. The evolutionary distances utilized to infer the phylogenetic tree have branch lengths scaled at 0.1.

3.2. Impact of mushroom biodegradation on PAP surface structure

Of the four mushrooms investigated, *Ganoderma lucidum* showed the most luxurious growth on PAP (Supplementary Figure 3), while the other mushrooms only grew sparsely. Scanning Electron Microscopy (SEM) analysis was performed to visualize structural changes caused by *G. lucidum* treatment. The PAP's SEM analysis can be used to qualitatively predict how sensitive the substrates will be to subsequent hydrolysis (Xu *et al*., 2017). The pretreatment resulted in more looseness and porosity in the cell wall structure of the PAP (Figure 2). There were visible fiber bundles after pretreatment, indicating that the biomass's structure was considerably broken down, indicating its suitability for hydrolysis.

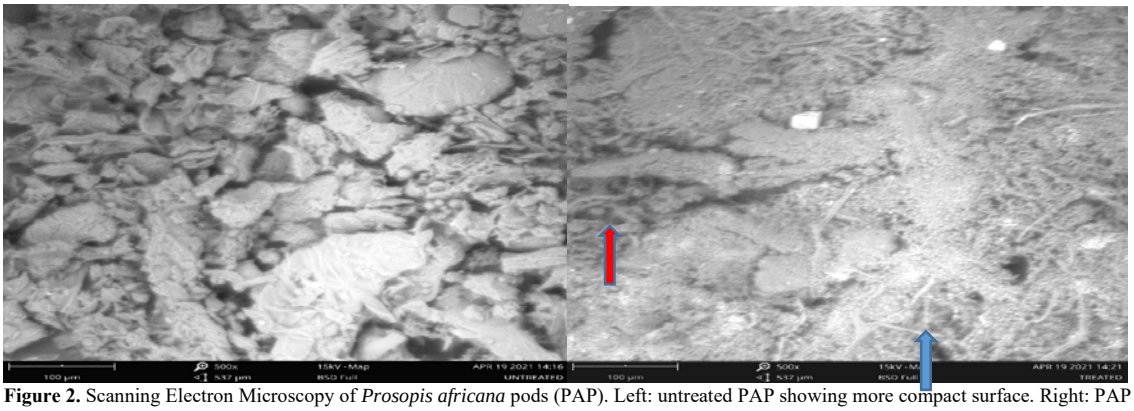

Figure 2. Scanning Electron Microscopy of *Prosopis africana* pods (PAP). Left: untreated PAP showing more compact surface. Right: PAP showing *Ganoderma lucidum*-pretreated PAP with hyphae (blue arrows) and fiber bundles (red arrow)

3.3. Optimisation of Dilute Acid Hydrolysis

The maximum concentration of reducing sugars, 43.37 ± 0.35 g/L, was found to be produced by 5 % HNO_3, 20 % solid loading, and a hydrolysis duration of 15 minutes (Supplementary Table 1). This value exceeds the 18.24 g/L that was obtained from the dilute acid hydrolysis of a similar substrate, *Prosopis juliflora* using 3 % dilute sulfuric acid (Gupta *et al*., 2009).

Figure 3 displays a parity plot that compares the experimental values of the response with those predicted by the statistical model. As a sign of good model fitness, the response points are all grouped together around the linear trendline.

The model's significance is demonstrated by the ANOVA result, which has a high F value of 270.95 and a p-value of 0.000 (Table 4). All the factors investigated had a significant effect on reducing sugar release as they all had p-values < 0.05. The interactions between all the analyzed factors were significant, from 2-way interactions to 4-way interactions.

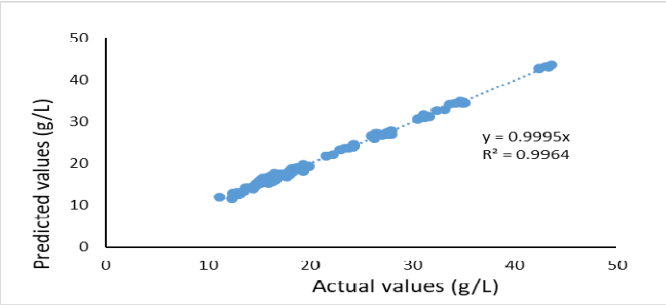

Figure 3: Parity plot of the predicted and actual reducing sugars concentrations from optimized dilute acid hydrolysis of PAP.

Table 4: ANOVA table for FFD model that describes sugar release from *Prosopis africana* pods (PAP) as a function of the chosen coefficient

Source	DF	Adj SS	Adj MS	F-Value	P-Value
Model	54	5900.57	109.27	270.95	0.000
Blocks	1	3.38	3.38	8.39	0.005
Linear	7	3732.52	533.22	1322.18	0.000
Acid type (A)	1	1832.41	1832.41	4543.68	0.000
Conc (%) (B)	2	907.92	453.96	1125.65	0.000
SLR (%) (C)	2	788.38	394.19	977.44	0.000
Time (mins) (D)	2	203.81	101.91	252.69	0.000
2-Way Interactions	18	1215.41	67.52	167.43	0.000
AB	2	305.71	152.85	379.02	0.000
AC	2	432.47	216.24	536.18	0.000
AD	2	7.28	3.64	9.03	0.000
BC	4	263.32	65.83	163.24	0.000
BD	4	83.46	20.87	51.74	0.000
CD	4	123.16	30.79	76.35	0.000
3-Way Interactions	20	617.05	30.85	76.50	0.000
ABC	4	185.63	46.41	115.07	0.000
ABD	4	100.90	25.23	62.55	0.000
ACD	4	95.37	23.84	59.12	0.000
BCD	8	235.14	29.39	72.88	0.000
4-Way Interactions	8	332.21	41.53	102.97	0.000
ABCD	8	332.21	41.53	102.97	0.000
Error	53	21.37	0.40		
Total	107	5921.94			

$R^2 = 0.9964$, R^2 (adj) = 0.9927

Sindhu *et al.* (2014) made similar observations, reporting that temperature, acid concentration, and time significantly affected reducing sugar release from biomass. The R^2 value of 0.9964, which shows that the model can account for 99.64 % of the response's variability, further supported the model's appropriateness.

3.4. Fermentation

A preliminary fermentation revealed that by Day 4 of growth, *P. kudriavzevii* SY4 produced a maximum concentration of ethanol of 27 g/L (data not shown).

3.4.1. Half-factorial screening of factors

A half-factorial design of experiment was used to assess the impact of temperature, inoculum size, pH, agitation speed, and fermentation time on ethanol production in order to increase yields from the preliminary fermentation (Table 2). Table 5 shows the variables, levels, and ethanol concentrations from the 32 runs of the screening fermentation.

Table 5: Half-factorial design screening of variables and outcomes

Run order	Temperature (oC)	Inoculum size (cells/ml)	pH	Agitation speed	Incubation period	Ethanol (g/L)
1	35	1 × 107	7	140	96	28.52
2	25	1 × 105	3	0	96	18.73
3	35	1 × 105	3	0	24	35.12
4	25	1 × 107	3	140	96	24.71
5	35	1 × 107	7	0	24	36.09
6	35	1 × 105	7	0	96	19.05
7	25	1 × 105	7	140	96	19.17
8	25	1 × 107	7	0	96	18.87
9	35	1 × 107	3	0	96	20.72
10	35	1 × 105	7	140	24	18.36
11	35	1 × 107	7	0	24	36.13
12	25	1 × 105	3	140	24	17.90
13	35	1 × 107	3	0	96	19.42
14	25	1 × 107	7	140	24	24.94
15	25	1 × 105	3	0	96	18.76
16	25	1 × 107	3	140	96	25.75
17	35	1 × 105	3	0	24	36.26
18	35	1 × 107	7	140	96	23.33
19	25	1 × 107	3	0	24	35.10
20	25	1 × 105	7	0	24	35.24
21	35	1 × 105	7	140	24	19.75
22	35	1 × 105	3	140	96	22.75
23	25	1 × 107	7	0	96	19.36
24	25	1 × 105	7	140	96	23.09
25	35	1 × 105	3	140	96	27.60
26	25	1 × 105	3	140	24	23.09
27	35	1 × 105	7	0	96	20.23
28	25	1 × 107	7	140	24	17.32
29	35	1 × 107	3	140	24	16.17
30	35	1 × 107	3	140	24	18.48
31	25	1 × 107	3	0	24	36.64
32	25	1 × 105	7	0	24	36.91

The Pareto chart indicated that inoculum size, pH, temperature, and their interactions had no significant effect on ethanol production (Fig. 4). pH not being significant in this screening contrasts with the findings of Dasgupta *et al.* (2013), who screened 9 factors in producing bioethanol from sugarcane bagasse pith hydrolysate and reported pH to be significant. It also differs with results of Wu (2019), who discovered pH to be a significant influence during the fermentation of bagasse hydrolysate that had been treated with an ionic liquid for the purpose of producing bioethanol. The presence of phenolic chemicals in PAP, which may have a buffering effect in the fermentation medium, may be the cause of the discrepancy in the results. Nonetheless, pH was further investigated over a wide range to confirm its influence on ethanol production from PAP hydrolysate.

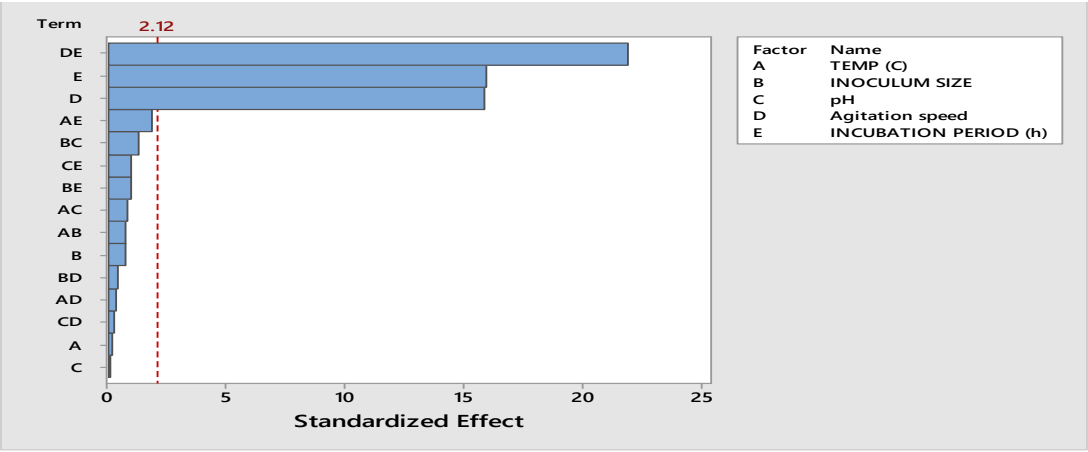

Figure 4. A Pareto chart displaying the factor's in their decreasing order of significance. At a 95% confidence level, bars that go beyond the vertical line represent statistically significant factors.

This study's results are in agreement with those of Karunakaran *et al.* (2013) in that temperature and inoculum size had no discernible impact on ethanol production. Agitation speed and incubation period significantly affected ethanol production (Figure 4), which is similar to the previously reported findings (Dasgupta *et al.*, 2013; Karunakaran *et al.*, 2013). A more effective conversion of carbohydrates to bioethanol is made possible by oxygen's favorable effects on the bioethanol fermentation process (Deniz *et al.*, 2014; Henriques *et al.*, 2018). The model had an R^2 value of 93.15 % with an R^2_{adj} of 91.83 %, implying that it can explain 93.15 % of the variability in ethanol production.

3.4.2. Factor optimization by RSM

RSM based on Box-Behnken design with 30 runs, was used to further analyze the two major components discovered through the screening experiment. pH was included as the third factor as RSM optimizations are accurately performed when three factors are investigated (Ahmed El-Imam *et al*., 2017). The BBD is a unique experimental design because treatment combinations frequently occur towards the edges of the experimental area. As a result, estimating the first and second-order coefficients is made simpler (Oiwoh *et al*., 2018).

The results of RSM optimization showed that pH 7, 70 rpm agitation, and 24 hours of fermentation were the ideal conditions for producing bioethanol from PAP diluted acid hydrolysate using *P. kudriavzevii* strain SY4. This produced a maximum bioethanol concentration of 38.26 ± 0.01 g/L (Table 6).

Table 6. The actual and predicted responses for the Box-Behnken Design matrix for the optimization of ethanol production from *Prosopis africana* pods dilute acid hydrolysate.

Run Order	pH	Agitation speed (rpm)	Incubation period (h)	Ethanol (g/L)	
				Actual	Predicted
1	5	70	60	21.47	21.99
2	5	140	24	34.04	33.70
3	7	140	60	31.28	31.85
4	7	70	96	24.32	24.88
5	5	0	24	32.44	31.78
6	5	70	60	24.68	24.99
7	3	0	60	26.12	26.70
8	3	70	96	29.49	29.16
9	5	0	96	24.61	27.71
10	3	140	60	21.50	22.50
11	3	70	24	27.97	28.72
12	5	70	60	26.55	25.99
13	7	0	60	26.39	26.97
14	7	70	24	38.26	37.62
15	5	140	96	29.94	27.48
16	7	70	96	32.04	31.91
17	5	0	24	29.17	29.81
18	3	70	24	30.94	30.75
19	5	140	24	28.70	27.73
20	5	70	60	24.83	25.01
21	5	140	96	27.02	27.50
22	5	70	60	27.44	26.01
23	3	140	60	22.78	22.52
24	5	70	60	25.03	25.01
25	7	0	60	28.31	27.99
26	5	0	96	31.54	31.74
27	3	70	96	27.61	29.19
28	3	0	60	21.87	21.73
29	7	70	24	38.25	37.64
30	7	140	60	23.88	27.87

Maximum bioethanol concentrations have been obtained under similar conditions (Betiku and Taiwo, 2015; Zani *et al*., 2019). However, the concentrations obtained were higher than those of Sivamani and Baskar (2018) and Dasgupta *et al*. (2013), with 25.59 g/L and 17.44 g/L, respectively, after similar optimization experiments. On the other hand, Techaparin *et al*. (2017) found that following BBD optimization, sweet sorghum juice had higher maximum bioethanol concentrations of 89.32 g/L. The results could differ depending on a number of things, including the biocatalyst, the type of substrate employed, and the fermentation conditions.

In order to determine how each factor affected the response, a quadratic equation was obtained:

$$\text{Ethanol (g/L)} = 34.52 + 0.51A - 0.0063B - 0.2917C + 0.120A^2 - 0.000056B^2 + 0.002926C^2 + 0.00279AB - 0.0195AC - 0.000012BC \quad (4)$$

According to the ANOVA results (Table 7), agitation speed had no discernible influence on bioethanol production, although pH and incubation time did. It was found that the incubation period was significant for the concentration of bioethanol while the square interactions of pH and agitation speed were not. It was also observed that the two-way interactions between all factors had no significant impact on bioethanol concentration. The lack of fit of 0.219 was insignificant, indicating the model's reliability. The model's robustness was measured with the R^2 value, which shows the quality of its prediction of responses. An R^2 value of 97.07 % and an R^2(adj) of 95.73 % indicates the model's suitability, as it can explain 97.07 % variability in response.

Table 7. ANOVA for the quadratic response surface model of ethanol production from *Prosopis africana* pods dilute acid hydrolysate

Source	DF	Adj SS	Adj MS	F-Value	P-Value
Model	10	191.918	19.192	3.87	0.005
Blocks	1	0.602	0.602	0.12	0.731
Linear	3	65.335	21.778	4.39	0.017
pH (A)	1	34.000	34.000	6.85	0.017
Agitation speed (rpm) (B)	1	0.059	0.059	0.01	0.914
Incubation period (h) (C)	1	31.276	31.276	6.31	0.021
Square	3	108.991	36.330	7.32	0.002
A2	1	1.688	1.688	0.34	0.566
B2	1	0.563	0.563	0.11	0.740
C2	1	106.211	106.211	21.41	0.000
2-Way Interaction	3	16.991	5.664	1.14	0.358
AB	1	1.225	1.225	0.25	0.625
AC	1	15.759	15.759	3.18	0.091
BC	1	0.007	0.007	0.00	0.971
Error	19	94.247	4.960		
Lack-of-Fit	15	84.429	5.629	2.29	0.219
Pure Error	4	9.818	2.455		
Total	29	286.165			

$R^2 = 0.9707$, R^2 (adj) = 0.9573

Additionally, three-dimensional response plots were created to display how the parameters affected the concentration of bioethanol (Figure 5)

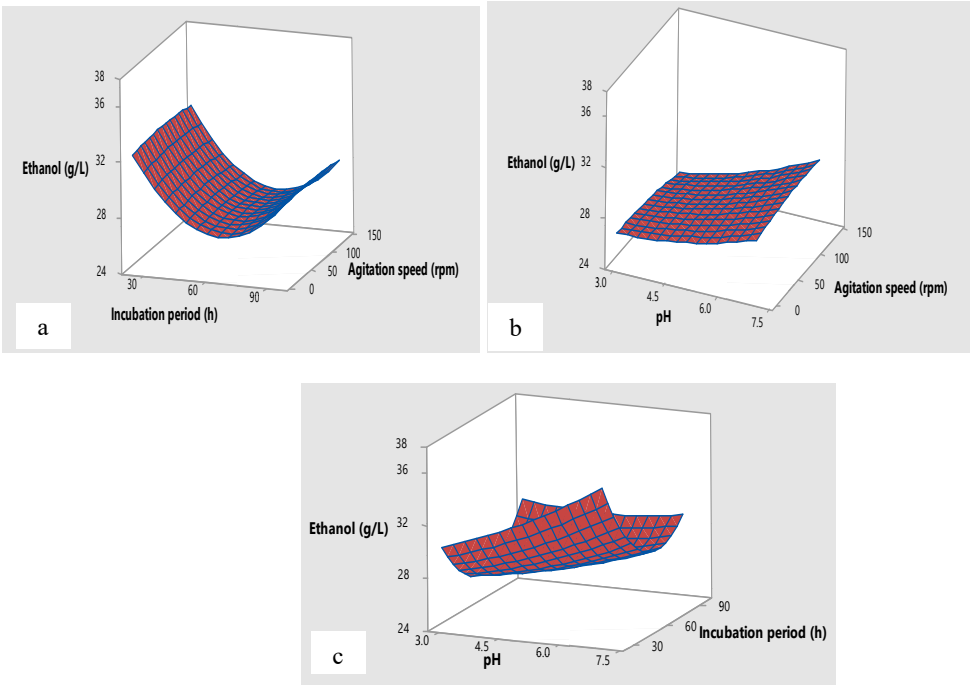

Figure 5: 3D surface plots illustrating how the concentration of bioethanol is affected by (a) incubation period and agitation speed, (b) agitation speed and pH, and (c) incubation period and pH.

The impact of agitation speed and incubation time on bioethanol concentration is depicted in Figure 5a. It was observed that within the range of factor levels tested, bioethanol concentration was higher at lower incubation time and agitation speed, reaching its peak at 24 hours and 70 rpm. Bioethanol concentration decreased with time, suggesting that this strain produces higher ethanol amounts early in the fermentation. The incubation time used in the screening experiments in this study appears to have missed the actual optimal time, which seems to be earlier than 24 hours. This is an advantageous finding as the lowered fermentation duration results in a lower cost of production, making the process economically competitive. A similar study involving the fermentation of hydrolyzed bagasse using a locally isolated yeast showed that peak ethanol concentrations were achieved at times earlier than 24 h (Hosny *et al*., 2016). These authors report that the progressive but minor reduction in ethanol concentration with time could be ascribed to evaporation or consumption of ethanol by the yeast. Higher agitation speeds could also result in faster ethanol evaporation.

Figure 5b shows the effect of pH and agitation speed on bioethanol concentration. It was observed that ethanol concentration increased with increasing pH, reaching its

peak at pH 7. Bioethanol concentration was higher at a lower agitation speed with a maximum concentration of 38.26 g/L at 70 rpm. Thus, higher rotation speed resulted in lower bioethanol concentration. The impact of pH and incubation time on bioethanol concentration is shown in Figure 5c. It was observed that high pH values resulted in higher bioethanol concentration.

Under the optimal conditions (pH 7.0, 70 rpm agitation, and 24 hours incubation time), 38.26 g/L of ethanol was produced, representing a 43.73 % increase in the product compared to unoptimised conditions. This increase can even be improved further at lower incubation times. These results show that PAP is a promising substrate that can be added to the mix of existing feedstocks currently exploited for bioethanol production.

4. Conclusion

Prosopis africana pod is an abundant and under-utilized food processing waste in Nigeria and other regions in Africa. This study showed that the biomass could support the luxurious growth of *Ganoderma lucidum*, which could increase Nigeria's production of the reishi mushroom. The affordable and mild biological pretreatment followed by statistically optimised dilute acid hydrolysis resulted in sugar-rich hydrolysates with up to 43.37 g/ L of sugars. This work is the first report of the hydrolysis requirements for *P. africana* pods and demonstrates its suitability for bioethanol production and other bioprocessing applications. It shows that efforts to exploit less common biomass types to produce bioethanol are still needed, particularly in the light of the Russia-Ukraine war, which has sent petroleum prices soaring globally.

References

Adelabu, B.A., Kareem, S.O., Oluwafemi, F., & Adeogun, I.A. (2017). Bioconversion of corn straw to ethanol by cellulolytic yeasts immobilized in *Mucuna urens* matrix. *J. King Saud Univ. Sci.,* 1-6.

Adelabu, B.A., Kreem, S.O., Adeogun, A.I., & Ademolu, K.O. (2018). Direct Bioconversion of Sorghum Straw to Ethanol in a Single-step Process by *Candida* species. *Jordan J. Biol. Sci.Jordan Journal of Biological Sciences,* **11(1):** 1-7.

Ahmed El-Imam, A., Akoh, P., Saliman, S., & Ighalo, E. (2021). Mushroom-mediated delignification of agricultural wastes for bio-ethanol production. *Niger. J. Biotechnol*., **38(1):** 137-145.

Ahmed El-Imam, A.M. (2017). Fermentative production of value-added products from sorghum bran. PhD thesis, University of Nottingham. Accessed from http://eprints.nottingham.ac.uk/43425/1/PHD%20THESIS.pdf. pp 14.

Ahmed El-Imam, A.M., Darren, G., Chenyu, D., & Paul, S.D. (2019). The development of a biorefining strategy for the production of biofuel from sorghum milling waste. *Biochem. Eng. J*., **150:** 107-288.

Atalla, S.M.M., Ahmed, N.E., Awad, H.M., El Gamal, N.G., & El Shamy, A.R. (2020a). Statistical optimization of xylanase production, using different agricultural wastes by *Aspergillus oryzae* MN894021, as a biological control of faba bean root diseases. *Egypt. J. Biol. Pest Control,* **30:** 125.

Atalla, S.M.M., EL Gamal, N.G., & Awad, H.M. (2020b). Chitinase of Marine *Penicillium chrysogenum* MH745129: Isolation, Identification, Production and Characterization as Controller for Citrus Fruits Postharvest Pathogens. *Jordan J. Biol. Sci.,* **13(1):** 19-28.

Atalla, S.M.M., EL Gamal, N.G., Awad, H.M., & Ali, N.F. (2019). Production of pectin lyase from agricultural wastes by isolated marine *Penicillium expansum* RSW_SEP1 as dye wool fiber. *Heliyon*, **5(8):** e02302.

Awoyale, A.A., & Lokhat, D. (2019). Harnessing the potential of bio-ethanol production from lignocellulosic biomass in Nigeria: A review, *Biofuels, Bioprod. Biorefining,* **13:** 192-207.

Awoyale, A.A., & Lokhat, D. (2021). Experimental determination of the effects of pretreatment on selected Nigerian lignocellulosic biomass in bioethanol production. *Sci. Rep*., **11:** 557.

Beig, B., Riaz, M., Naqvi, S.R., Hassan, M., Zheng, Z., Karimi, K., Pugazhendhi, A., Atabani, A.E., & Chi, N.T.L. (2021). Current challenges and innovative developments in pretreatment of lignocellulosic residues for biofuel production: A review. *Fuel,* **287:** 119670.

Betiku, E., & Taiwo, A.E. (2015). Modeling and Optimization of bioethanol production from breadfruit starch hydrolyzate vis-a-vis response surface methodology and artificial neural network. *Renew. Energ.* **74:** 87-94.

Bhatia, S.K., Kim, S.H., Yoon, J.J., & Yang, Y.H. (2017). Current status and strategies for second generation biofuel production using microbial systems. *Energy Convers. Manag.,* **148:** 1142-1156.

Branco, R.H., Serafim, L.S., & Xavier, A.M. (2019). Second generation bioethanol production: on the use of pulp and paper industry wastes as feedstock. *Fermentation,* **5(1):** 4.

Braz, A., Mateus, M.M., dos Santos, R.G., Machado, R., Bordado, J.M., & Correia, M.J.N. (2019). Modelling of pine wood sawdust thermochemical liquefaction. *Biomass Bioenergy,* **120:** 200-210.

Chang, Y.H., Chang, K.S., Chen, C.Y., Hsu, C.L., Chang, T.C., & Jang, H.D. (2018). Enhancement of the efficiency of bioethanol production by *Saccharomyces cerevisiae* via gradually batch-wise and fed-batch increasing the glucose concentration. *Fermentation,* **4:** 45.

da Silva, C.G.M., Andrade, S.A.C., Schuler, A.R.P., de Souza, E.L., & Stamford, T.L.M. (2011). Production of ethanol from mesquite [*Prosopis juliflora* (SW) D.C.] pods mash by *Zymomonas mobilis* in submerged fermentation. *Sci. Agric*., **68(1):** 124–127.

Dasgupta, D., Suman, S.K., Pandey, D., Ghosh, D., Khan, R., Agrawal, D., Jain, R.K., Vadde, V.T., & Adhikari, D.K. (2013). Design and Optimization of ethanol production from bagasse pith hydrolysate by a thermotolerant yeast *Kluyveromyces* sp. IIPE453 using response surface methodology. *Springerplus,* **2:** 159.

Deniz, I., Imamoglu, E., & Vardar-Sukan, F. (2014). Aeration-enhanced bioethanol production. *Biochem. Eng. J.,* **92:** 41–46.

Gerbens-Leenes, P. (2017). Bioenergy water footprint, comparing first, second and third generation feedstocks for bioenergy supply in 2040. *Eur. Water,* **59:** 373-380.

Ghani, H.U., Silalertruksa, T., & Gheewala, S.H. (2019). Water-energy food nexus of bioethanol in Pakistan: a life cycle approach evaluating footprint indicators and energy performance. *Sci. Total Environ.,* **687:** 867–876.

Gupta, R., Sharma, K.K., & Kuhad, R.C. (2009). Separate hydrolysis and fermentation (SHF) of *Prosopis juliflora*, a woody substrate, for the production of cellulosic ethanol by *Saccharomyces cerevisiae* and *Pichia stipitis*-NCIM 3498. *Bioresour. Technol*., **100(3):** 1214–1220.

Gustin, G. (2022). As Russia's War In Ukraine Disrupts Food Production, Experts Question the Expanding Use of Cropland for

Biofuels. *Inside Climate News.* Retrieved from https://insideclimatenews.org/news/05042022/as-russias-war-in-ukraine-disrupts-food-production-experts-question-the-expanding-use-of-cropland-for-biofuels/ (2022, April 5).

Hamed, E.R., Awad, H.M., Ghazi, E.A., El-Gamal, N.G., & Shehata, H.S. (2015). *Trichoderma asperellum* isolated from salinity soil using rice straw waste as biocontrol agent for cowpea plant pathogens. *J. Appl. Pharm. Sci*., **5(2):** 91–98

Henriques, T.M., Pereira, S.R., Serafim, L.S., & Xavier, A.M.R.B. (2018). Two-Stage Aeration Fermentation Strategy to Improve Bioethanol Production by *Scheffersomyces stipitis*. *Fermentation*, **4(4):** 97.

Hosny, M., Abo-State, M.A., El-Temtamy, S.A., & El-Sheikh, H.H. (2016). Factors affecting bioethanol production from hydrolyzed bagasse. *Int. J. Adv. Res. Biol. Sci.*, **3(9):** 130-138.

I.E.A. (2019). Renewables 2019. Paris: IEA. Document Number)---. (2020). Global Energy Review 2020. Paris: IEA. Document Number)

Ibeto, C., Ofoefule, A., & Agbo, K. (2011). A global overview of biomass potentials for bioethanol production: a renewable alternative fuel. *Trends Appl. Sci. Res.,* **6:** 410-425.

Iticha, T.N. (2016). Isolation and screening of ethanol tolerant yeast for bioethanol production in Ethiopia. *GJLSBR*., **2(2):** 1-7.

Karimi, K., Shafiei, M., & Kumar, R. (2013). Progress in physical and chemical pretreatment of lignocellulosic biomass. Biofuel Technologies. Berlin: Springer, Berlin, Heidelberg.

Karunakaran, S., Ramasamy, G., Duraisamy, S., & Balakrishnan, S. (2013). Screening and Optimization of fermentation media for increased production of ethanol from *Gracilaria* sp. Using Response Surface Methodology. *J. Pure Appl. Microbiol.,* **7(4):** 2641-2652.

Koshy, B.E., Pandey, F.K., & Bhatnagar, T. (2014). Quantitative estimation of bioethanol produced from lignocellulosic & household wastes. *Int. J. Life Sci. Res.* **2(4):** 130-145.

Malik, K., Salama, E., Kim, T.H., & Li, X. (2020). Enhanced ethanol production by *Saccharomyces cerevisiae* fermentation post acidic and alkali chemical pretreatments of cotton stalk lignocellulose. *Int. Biodeterior. Biodegrad.,* **147:** 104869.

Manavalan, T., Manavalan, A., & Heese, K. (2015). Characterization of lignocellulolytic enzymes from white-rot fungi. *Curr. Microbiol.,* **70:** 485-498.

Milano, J., Ong, H., Masjuki, H., Chong, W., Lam, M.K., Loh, P.K., & Vellayan, V. (2016). Microalgae biofuels as an alternative to fossil fuel for power generation. *Renew. Sustain. Energy Rev.,* **58:** 180-197.

Oiwoh, O., Ayodele, B.V., Amenaghawon, N.A., & Okieimen, C.O. (2018). Optimization of bioethanol production from simultaneous saccharification and fermentation of pineapple peels using *Saccharomyces cerevisiae*. *J. Appl. Sci. Environ. Manage.,* **22(1):** 54-59.

Oni, O.D., Oke, M.A., & Sani, A. (2020). Mixing of *Prosopis africana* pods and corn cob exerts contrasting effects on the production and quality of *Bacillus thuringiensis* crude endoglucanase. *Prep. Biochem. Biotechnol.*, 1–10.

Pasiecznik, N.M., Tewari, J.C., Harsh, L.N., Felker, P., Harris, P.J.C., Cadoret, K., Cruz, G., & Maldonado, L.J. (2001). The *Prosopis juliflora - Prosopis pallida* Complex: A Monograph. Henry Doubleday Research Association (HDRA): Coventry, UK.

Raina, N., Slathia, P.S., & Sharma, P. (2020). Response surface methodology (RSM) for Optimisation of thermochemical pretreatment method and enzymatic hydrolysis of deodar sawdust (DS) for bioethanol production using separate hydrolysis and co-fermentation (SHCF). *Biomass Conv. Bioref.* https://doi.org/10.1007/s13399-020-00970-0.

Rani, P., Kalyani, N., & Prathiba, K. (2008). Evaluation of Lignocellulosic Wastes for Production of Edible Mushrooms. *Appl. Biochem. Biotechnol.*, **151:** 151–159.

Rezania, S., Oryani, B., Cho, J., Talaiekhozani, A., Sabbagh, F., Hashemi, B., Rupani, P.F., & Mohammadi, A.A. (2020). Different pretreatment technologies of lignocellulosic biomass for bioethanol production: an overview. *Energy,* 117457.

Sana, H., Kanwal, S., Akhtar, J., Haider, R., Nawaz, S., Sheikh, N., & Munir, S. (2017). Production of ethanol and bio-chars from Pakistani lignocellulosic biomasses. *Energy Sources A: Recovery Util. Environ. Eff.,* **39(5):** 465-472.

Sindhu, R., Binod, P., & Pandey, A. (2016). Biological pretreatment of lignocellulosic biomass–An overview. *Bioresour. Technol.*, **199:** 76-82.

Sindhu, R., Kuttiraja, M., Binod, P., Sukumaran, R.K., & Pandey, A. (2014). Bioethanol production from dilute acid pretreated Indian bamboo variety (*Dendrocalamus* sp.) by separate hydrolysis and fermentation. *Ind. Crops Prod.,* **52:** 169–176.

Sivamani, S., & Baskar, R. (2018). Process design and optimization of bioethanol production from cassava bagasse using statistical design and genetic algorithm. *Prep. Biochem. Biotechnol.*, DOI: 10.1080/10826068.2018.1514512.

Tamura, K., Peterson, D., Peterson, N., Stecher, G., Nei, M., & Kumar, S. (2011). MEGA5: molecular evolutionary genetics analysis using maximum likelihood, evolutionary distance, and maximum parsimony methods. *Mol. Biol. Evol.*, **28(10):** 2731–2739.

Taufikurahman, T., Jessica, S., & Delimanto, W.O. (2020). A comparison of alkali and biological pretreatment methods in napier grass (*Pennisetum purpureum* Scumach.) for reducing lignin content in the bioethanol production process. *J. Biol. Sci. Technol Manag.,* **2(1):** 31-43.

Techaparin, A., Thanonkeo, P., & Klanrit, P. (2017). High-temperature ethanol production using thermotolerant yeast newly isolated from Greater Mekong Subregion. *Braz. J. Microbiol.*, **238:** 1-15.

Wu, Z. (2019). Mixed fermentation of *Aspergillus niger* and *Candida shehatae* to produce bioethanol with ionic-liquid-pretreated bagasse. *3 Biotech* **9:** 41.

Wuryantoro, W., Adinurani, P.G., Wardhani, R.M., Sutrinso, S., Yamin, B.M., & Nur, S.M. (2021). Utilization of "Uwi" Plant (_Dioscorea_ sp.) as a Renewable Bioenergy Resource. *Jordan J. Biol. Sci.Jordan Journal of Biological Science,* **14(5):** 945-951.

Xie, T., Liu, J., Du, K., Liang, B., & Zhang, Y. (2013). Enhanced biofuel production from high-concentrated bioethanol wastewater by a newly isolated heterotrophic microalga, *Chlorella vulgaris* LAM-Q. *J. Microbiol. Biotechnol.,* **23(10):** 1460-1471.

Xu, X., Xu, Z., Shi, S., & Lin, M. (2017). Lignocellulose degradation patterns, structural changes, and enzyme secretion by *Inonotus obliquus* on straw biomass under submerged fermentation. *Bioresour. Technol.,* **241:** 415-423.

Yildirim, O., Ozkaya, B., Altinbas, M., & Demir, A. (2021). Statistical Optimization of dilute acid pretreatment of lignocellulosic biomass by response surface methodology to obtain fermentable sugars for bioethanol production. *Int. J. Energy Res.,* **45(6):** 8882–8899.

Zani, S.H.M., Asri, F.M., Azmi, N.S., Yussof, H.W., & Zahari, M.A.K.M. (2019). Optimization of process parameters for bioethanol production from oil palm frond juice by Saccharomyces cerevisiae using Response Surface Methodology as a tool. Mater. Sci. Eng., 702: 012003.

APPENDIX

Supplementary Table 1: Full-factorial experimental design and results obtained for dilute acid hydrolysis

Run Order	Acid type	Conc (%)	SLR (%)	Time (mins)	Reducing sugars (g/L)	
					Actual	Predicted
1	HNO3	3	10	15	26.23	26.46
2	HNO3	3	10	60	42.38	42.65
3	H3PO4	1	20	15	17.20	17.07
4	HNO3	3	20	15	33.63	34.17
5	HNO3	5	5	15	17.39	17.52
6	H3PO4	1	5	60	12.82	12.65
7	HNO3	3	20	30	34.71	34.97
8	H3PO4	1	10	30	16.72	16.47
9	HNO3	1	20	30	24.25	24.10
10	H3PO4	3	20	15	18.80	18.54
11	HNO3	3	10	30	30.50	30.70
12	HNO3	5	20	30	32.42	32.59
13	H3PO4	5	5	15	22.88	23.17
14	HNO3	5	10	15	34.14	34.38
15	HNO3	3	5	60	14.31	14.34
16	HNO3	5	20	60	31.61	31.20
17	HNO3	5	20	15	43.12	43.19
18	HNO3	1	20	60	17.96	18.23
19	H3PO4	1	20	60	14.45	13.90
20	H3PO4	5	20	60	17.98	17.82
21	H3PO4	5	5	60	12.46	12.88
22	H3PO4	5	10	60	16.27	16.01
23	H3PO4	1	10	15	14.81	15.07
24	H3PO4	3	5	15	17.12	17.00
25	HNO3	1	10	30	21.60	21.74
26	H3PO4	3	5	60	12.37	11.55
27	HNO3	5	10	60	26.26	26.47
28	H3PO4	3	10	30	19.92	19.43
29	HNO3	5	10	30	27.52	27.54
30	H3PO4	3	20	60	13.02	12.55
31	H3PO4	5	20	15	15.35	16.37
32	H3PO4	3	10	15	16.10	16.86
33	H3PO4	1	10	60	15.21	15.29
34	HNO3	3	5	30	23.35	23.52
35	H3PO4	5	5	30	18.80	18.47
36	H3PO4	3	20	30	16.26	16.87
37	H3PO4	5	10	30	17.01	17.49
38	HNO3	1	20	15	18.14	18.71
39	HNO3	3	5	15	17.13	17.39
40	H3PO4	3	5	30	16.83	17.58
41	H3PO4	5	20	30	26.01	26.58
42	HNO3	1	5	30	18.12	18.20
43	HNO3	1	5	60	16.91	16.93
44	HNO3	1	10	15	18.67	18.61
45	HNO3	5	5	30	23.00	23.19
46	HNO3	1	5	15	15.17	15.93
47	H3PO4	5	10	15	18.85	18.80
48	HNO3	1	10	60	14.70	15.03
49	H3PO4	1	5	30	14.99	15.65
50	HNO3	5	5	60	19.12	18.98
51	H3PO4	1	5	15	13.30	13.12
52	H3PO4	1	20	30	15.06	15.69
53	HNO3	3	20	60	26.45	27.38
54	H3PO4	3	10	60	16.51	17.75
55	HNO3	1	5	15	16.34	15.58
56	H3PO4	3	10	15	17.98	17.22
57	HNO3	3	5	60	14.72	14.69
58	HNO3	1	5	60	17.30	17.28
59	HNO3	3	5	30	24.05	23.88
60	HNO3	1	20	30	24.30	24.45
61	H3PO4	5	5	60	12.94	12.52
62	HNO3	3	10	15	26.33	26.10
63	H3PO4	3	20	60	12.44	12.91
64	HNO3	3	10	60	43.28	43.01
65	H3PO4	1	20	30	16.67	16.04
66	H3PO4	5	5	30	18.50	18.83

67	HNO3	5	10	30	27.91	27.89
68	HNO3	3	10	30	31.25	31.05
69	HNO3	5	5	60	18.48	18.62
70	H3PO4	3	5	60	11.09	11.91
71	H3PO4	1	5	60	12.83	13.00
72	H3PO4	5	10	60	16.10	16.36
73	H3PO4	1	10	15	15.68	15.42
74	H3PO4	5	10	15	19.11	19.16
75	H3PO4	1	10	30	16.57	16.82
76	H3PO4	1	5	15	13.48	13.30
77	HNO3	5	20	30	33.12	32.95
78	HNO3	3	20	30	34.87	34.61
79	H3PO4	3	20	30	17.83	17.22
80	H3PO4	5	10	30	18.32	17.84
81	H3PO4	3	10	30	19.30	19.79
82	H3PO4	5	20	30	27.51	26.94
83	H3PO4	3	10	60	19.35	18.11
84	HNO3	5	5	30	23.74	23.55
85	HNO3	3	20	60	27.95	27.02
86	H3PO4	1	5	30	15.96	15.30
87	H3PO4	3	20	15	18.63	18.89
88	H3PO4	5	20	60	18.01	18.17
89	HNO3	1	10	30	22.24	22.10
90	H3PO4	1	10	60	15.72	15.64
91	HNO3	1	10	60	15.72	15.39
92	HNO3	1	20	15	18.93	18.36
93	HNO3	5	20	60	31.14	31.55
94	HNO3	5	10	60	27.04	26.83
95	HNO3	5	20	15	43.62	43.55
96	HNO3	1	10	15	18.90	18.96
97	H3PO4	5	20	15	17.74	16.72
98	H3PO4	1	20	60	13.70	14.25
99	HNO3	3	20	15	35.06	34.52
100	H3PO4	3	5	15	17.23	17.35
101	HNO3	3	5	15	18.01	17.75
102	H3PO4	5	5	15	23.82	23.53
103	HNO3	1	20	60	18.86	18.59
104	HNO3	5	5	15	18.01	17.88
105	H3PO4	3	5	30	17.98	17.23
106	HNO3	5	10	15	34.97	34.73
107	HNO3	1	5	30	18.63	18.55
108	H3PO4	1	20	15	17.29	17.42

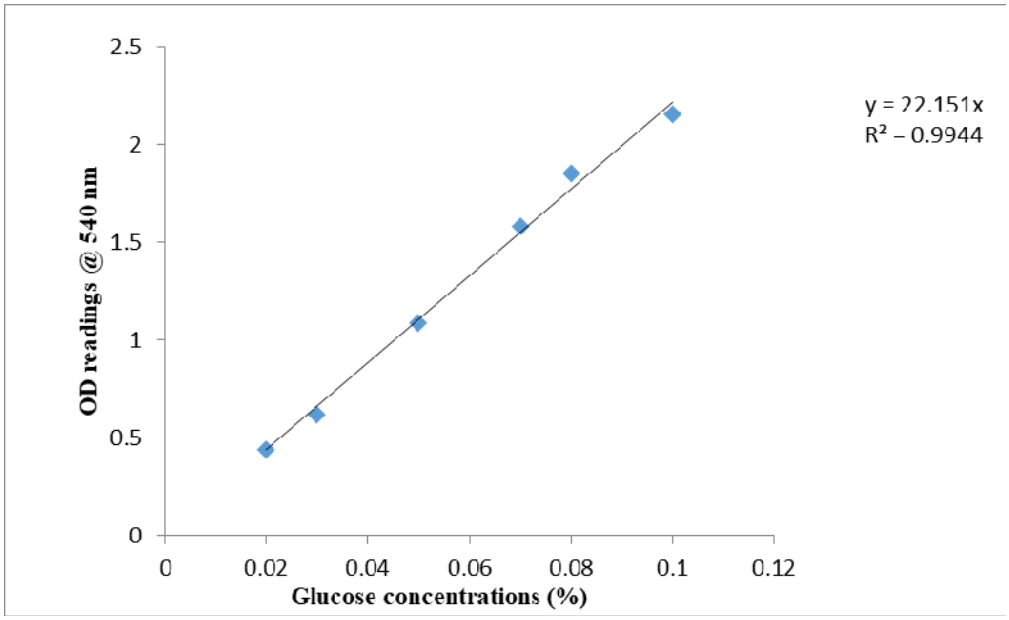

Supplementary Figure 1: Glucose standard curve

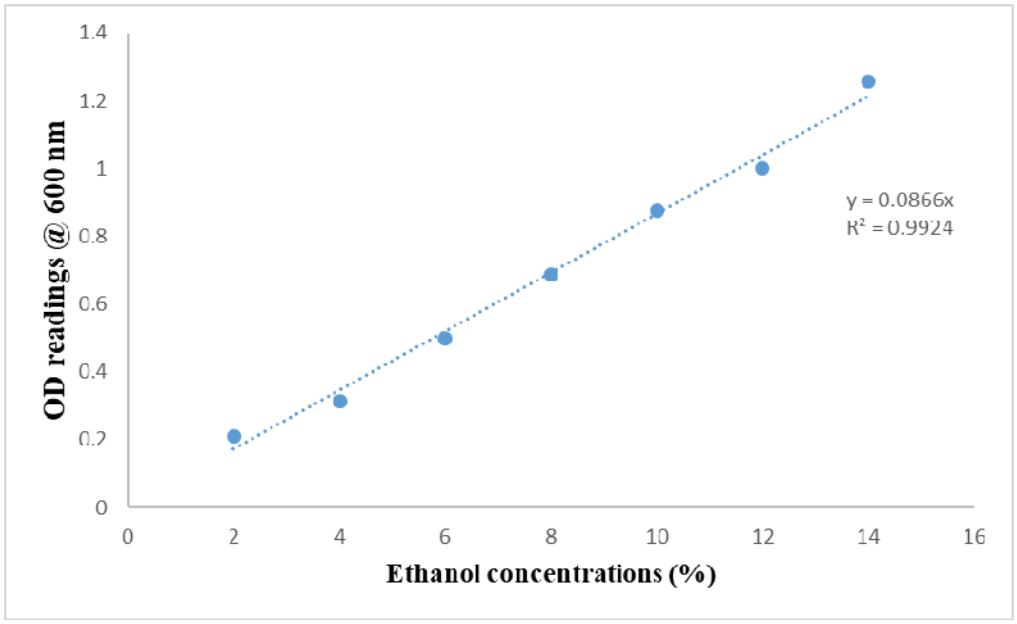

Supplementary Figure 2: Ethanol standard curve

Supplementary Figure 3: Growth pattern of *Ganoderma lucidum* on milled *Prosopis africana* pods.